QUANTIFYING THERMAL EXPOSURES AND EFFECTS FOR CENTRAL VALLEY ANADROMOUS SALMONIDS

Authors: Alyssa FitzGerald, Sara John, Travis Apgar, and Benjamin Martin
University of California, Santa Cruz Agreement #16-048-150

TABLE OF CONTENTS

ABSTRACT

Temperature directly and indirectly controls biophysical, biochemical, and bioenergetic processes and is the primary abiotic factor that influences ectotherms via their spatial distributions, daily and long-term survival, and evolutionary trajectory. Here we examine temperature exposure and effects on survival of multiple life stages of Chinook salmon, a species that is economically important but declining. Although thermal criteria are defined for Pacific Northwest populations, it is unclear if these criteria are appropriate for California populations at the southern extreme of the species. We first quantify the thermal environment experienced by Central Valley salmonid populations in the context of Pacific Northwest populations. To do this, we 1) expanded a pre-existing spatial stream network model to all months of the year, predicting mean monthly temperature for nearly every river km in the western U.S., 2) developed a phenology database for each life stage of each population, and 3) defined spatial distributions of each life stages for each population. We found that Central Valley populations were exposed to significantly higher temperatures during peak holding, peak incubation, and early juvenile growth compared to many Pacific Northwest populations, and these temperatures were sometimes well above the Region 10 thermal criteria, especially for Central Valley spring-run during holding and Sacramento River winter-run during incubation. We next demonstrate a framework that provides a quantitative approach for assessing incremental changes in temperature on survival in Central Valley rivers across runs and life stages. We found that spring-run were more thermally vulnerable than fall-run, perhaps explaining why Central Valley spring-run are an ESA-listed population. A comparison across life stages revealed that temperature-dependent mortality during holding is more limiting for the populations examined here than embryonic mortality or juvenile mortality. We conclude by discussing additional studies that are required in order to define California-specific thermal criteria. Until then, we recommend using our approach to better manage site-specific populations in the Central Valley.

INTRODUCTION TO PROJECT

Temperature is a major controlling factor of biophysical, biochemical, and bioenergetic processes (Fry 1971). For ectotherms, temperature is the primary abiotic factor that influences spatial distributions (Fourcade et al. 2018), physiological rates, daily and long-term survival, and evolutionary trajectory (Brannon et al. 2004). Seasonal patterns in temperature have resulted in corresponding life-history patterns for aquatic species, shaping the traits of populations and thereby affecting responses and sensitivity to temperature changes (Quinn 2005, Flitcroft et al. 2016, Nadeau et al. 2017). Examining temperature exposure and effects on different populations is therefore of paramount importance to define trait diversity among populations and predict differential responses to changing temperature regimes.

Pacific salmonids are economically and commercially important (NRC 1996), but, in general, populations have been declining due to habitat degradation and alteration, over-harvesting, and the elimination of thermally suitable habitat from dams (Moyle 2002, Moyle et al. 2017). Water temperature is the primary factor affecting salmonid survival and evolution in freshwater habitats (Roper and Scarnecchia 1999, Poole et al. 2001, Todd et al. 2008, Isaak et al. 2017a), and populations have likely adapted to the long-term historic thermal regime average (Quinn 2005). Because Chinook are semelparous, reproducing a single time, there is immense selective pressure on the spatial structuring and phenology of their freshwater life stages. For example, eggs spawned too far upstream where temperatures are cold may take too long to develop whereas eggs spawned in warmer reaches may experience lethal temperatures (downstream, generally). However, much of the former spawning habitat of Central Valley salmonids is blocked by dams, constraining the freshwater life stages of these populations to lower elevation, warmer habitat (Lindley et al. 2004, Moyle et al. 2017).

Dams and warming stream temperatures have resulted in exposure to novel temperature regimes for which salmon are not adapted. These novel temperature regimes may result in decreased survival unless populations can track historic temperature regimes by shifting their spatial distribution and/or phenology, physiologically adapt to warmer temperatures, or have humans intervene by managing for historically ideal stream temperatures. To mimic the thermal regimes of former habitat, managers can release cold water from reservoirs above dams. The temperature target for each life stage is based on the United States Environmental Protection Agency (USEPA) – Region 10 Guidance for Pacific Northwest State and Tribal Temperature Water Quality Standards (U.S. Environmental Protection Agency 2003).

A central part of this project is to determine whether Region 10 temperature criteria that were derived for salmonid populations in Oregon, Washington, Idaho, and Alaska (U.S. EPA 2003) are appropriate for salmonid populations in California. In other words, are California populations physiologically and behaviorally adapted to the thermal environments at the southernmost edge of their distribution? Although there are several examples of salmonid populations physiologically adapting to their local thermal regime (e.g. Eliason et al. 2011, Poletto et al. 2017), a recent review found a paucity of data to compare the thermal tolerance of California vs. region 10 populations (Zillig et al. in prep). Here we describe a set of modeling research tasks that – combined with the comparative laboratory and field studies recommended by Zillig et al. (in prep.) – will define thermal exposure and help calculate the effects of temperature on different life stages of anadromous salmonid populations in the Central Valley. This work will be the first step to determine if Region 10 criteria are applicable to the Central

Valley. When Region 10 thresholds cannot be met during particularly warm years, our framework will allow managers to compare thermal effects on different life stages in order to assess which life stages are the most vulnerable in space and time. Our work addresses three main research questions:

Q1. How can we quantify the thermal environment experienced by Central Valley salmonid populations, and how does it differ from Region 10 populations?

Q2. Can we improve site-specific temperature management in the Central Valley by using thermal performance curves?

Q3. What additional studies are needed in order to develop specific thermal thresholds for the different life stages of salmonids in the Central Valley?

To answer these questions, we need to know where (distribution) and when (phenology) different life stages of each population occurs, and what stream temperatures are associated with these life stages in space and time. Below, we describe our methodology behind the first two questions, provide examples using Chinook populations from the Central Valley, and discuss future analyses and implications. We end by providing recommendations of future studies required in order to establish site-specific thermal thresholds for salmonids in the Central Valley.

Part 1. How can we quantify the thermal environment experienced by Central Valley salmonid populations, and how does it differ from Region 10 populations?

INTRODUCTION

In comparison with northerly populations, southern salmonids are exposed to warmer temperatures and more variable weather events. Whether salmonid populations are negatively impacted by these elevated temperatures depends in large part on the degree to which populations have adapted to their local thermal environments. An important first step in quantifying the degree of thermal adaptation of California salmonid populations is to quantify how the thermal environment they experience differs from Region 10 populations. Comparisons of local studies tend to support the assumption that thermal exposure varies between ESUs, but a range-wide assessment of all ESUs for multiple life stages has not been undertaken. Comparison of populations in individual rivers (e.g. Sacramento River and Snake River) is overly simplistic and can miss broad spatial patterns, so here we analyze spatial and temporal patterns in temperature exposure for Central Valley populations in the context of all other populations in Region 10.

Quantifying the thermal exposure for highly mobile salmonid populations is difficult for several reasons. First, temperature in river networks is highly dynamic in time and space, but temperature data is sparse – a very small fraction of the hundreds of thousands of river km in the western U.S. have observed temperature data. Secondly, salmon populations move through these dynamic networks in space and time in complex ways. Finally, because different life stages of salmon populations have different thermal sensitivities, and the thermal exposure of each life stage depends on the life stage preceding it in time and space, a detailed understanding of both the distribution and phenology of each life stage is required. We overcome these challenges by 1) applying a statistical stream network model that translates sparse temperature data into monthly stream temperature predictions for every river km in the western U.S., 2) aggregating presence points and distributions from multiple data sources to create the most complete distribution dataset possible for each life stage of each population, and 3) developing a database of the phenology of each life stage of each population.

The distribution and phenology databases allow us to examine spatial and temporal patterns for each ESU, run, and life stage. To examine spatial and temporal temperature patterns between different groupings, i.e. different life stages within and between populations, we overlaid our distribution and phenology datasets with stream temperature. By comparing expected thermal exposures using a generic vs. population-specific phenology, we quantify the degree to which phenology buffers exposures to elevated temperatures for California populations. Finally, we quantify thermal exposure for California populations compared to those in Region 10, and determine which life-stages/runs/rivers within the Central Valley are exposed to temperatures near the Region 10 thresholds and may therefore be more vulnerable to incremental increases in temperature.

METHODS

Datasets

Phenology database

　　We reviewed primary and secondary literature sources to develop a phenology database for each life history stage of each population (Appendix 1 Table S1.1, Appendix 1 List 1). If a recognized ESU contains multiple runs, we separated runs due to phenological differences and hereafter refer to all such groupings as populations. Our database is on a monthly time-step to match the temporal resolution of the stream temperature dataset. The peak month (or median if peak was unknown) of each life stage was defined. We joined the table to ESU distributions in ArcGIS and plan to make this dataset and its metadata (including sources) publicly available.

Distribution dataset

　　The distribution dataset defines spatial distributions of life stages for different populations. Occurrences were extracted August 2017-January 2018 from eight field-observational and distributional data sources[1]. Linear distribution datasets (StreamNet and CalFish) were broken up into points separated by 1 km, then added to the observational dataset. Occurrences are accurate to 500 m, and each occurrence was defined by populations (i.e. unique ESU/run combination), life stage, and month. Fish of unknown population, unknown life stage, or known hatchery origin were removed. To match the temporal limit of the stream temperature modeling project, occurrences prior to 1993 were removed. We defined the ESU (if not specified) by spatially merging occurrences with ESUs (http://www.westcoast.fisheries.noaa.gov/maps_data/Species_Maps_Data.html). Due to low numbers and ambiguity of other life stages (e.g. "juvenile" could indicating rearing or outmigration), we focused our efforts on occurrences listing spawning location, such as those based on redd counts or spawner surveys, and defined holding, incubation, and early rearing at these locations. Duplicate observations were removed using R. This filtering resulted in a total of 52,261 occurrences (Fig. 1).

Monthly stream temperature

　　Obtaining stream temperature involved expanding a pre-existing spatial stream network model (SSN) (Isaak et al. 2017), currently only available for August, to all months of the year in order to have a full picture of the habitat that is thermally available to salmonids at various life stages. SSNs have been shown to be an effective modeling strategy for stream temperature because they are able to account for the complex autocovariance structures inherent to stream temperature data (Peterson and Ver Hoef 2010, Rushworth et al. 2015, Isaak et al. 2017). Following Isaak et al. (2017), our SSN models includes three autcovariance functions: tail-down, tail-up, and Euclidean distance. Tail-down autocovariance functions are based on moving average functions in the downstream direction and allow correlation between sites that are flow-

---

[1] ASOD: obtained via California Dept. of Fish and Wildlife
CalFish: http://www.calfish.org/DataandMaps/CalFishDataExplorer.aspx
Global Biodiversity Information Facility: www.gbif.org
OBIS: www.iobis.org
StreamNet: https://www.streamnet.org/
U.S. EPA: https://www.epa.gov/national-aquatic-resource-surveys/data-national-aquatic-resource-surveys
U.S.G.S.: https://aquatic.biodata.usgs.gov
VertNet: http://vertnet.org/

connected and sites that are flow-unconnected (Ver Hoef and Peterson 2010). Tail-up autocovariance functions are based on moving average functions in the upstream direction, allow correlation between sites that are connected by flow, and use spatial weighting to partition the moving average function at tributary confluences (Ver Hoef and Peterson 2010). An autocovariance function based on Euclidian distance ("as the bird flies") is used to account for sources of autocorrelation not attributable to the network structure of rivers. Research has shown advantages in using a mixed model approach which combines multiple autocovariance functions (Peterson and Ver Hoef 2010).

We are expanding the results of Isaak et al. (2017) to multiple months of the year, and below is a summary of the SSN model. The model has the form:

$$y = X\beta + L\gamma + R\eta + z_{TU} + z_{TD} + z_{EUC} + \varepsilon$$

where y is a vector of observed water temperatures; X is a design matrix of covariate values; β is a vector of regression coefficients; L is a random-effects design matrix for location; γ is a vector of zero-mean, normally distributed random effects for location; R is a random-effects design matrix for year; η is a vector of zero-mean, normally distributed effects for year; z_{TU}, z_{TD}, and z_{EUC} are vectors of zero-mean random effects with an autocorrelation structure based on an exponential tail-up function with spatial weights determined by watershed area, an exponential tail-down function, and an exponential Euclidian function, respectively; and ε is a vector of independent and normally distributed random errors. The covariance matrix is given by:

$$\Sigma = \sigma^2_\gamma LL' + \sigma^2_\eta RR' + \sigma^2_{TU}C_{TU} + \sigma^2_{TD}C_{TD} + \sigma^2_{EUC}C_{EUC} + \sigma^2_\varepsilon I$$

where σ^2_γ, σ^2_η, σ^2_{TU}, σ^2_{TD}, σ^2_{EUC}, and σ^2_ε are variances for γ, η, z_{TU}, z_{TD}, z_{EUC}, and ε, respectively, and C_{TU}, C_{TD}, and C_{EUC} are autocorrelation matrices for z_{TU}, z_{TD}, z_{EUC}, respectively, where each C-matrix has an additional parameter that controls the spatial range of autocorrelation for that model, and I is the identity matrix.

SSN models require a stream network, observed water temperatures at discrete locations, and spatially and/or temporally explicit covariates. This model uses the National Stream Internet (NSI) network, which was derived from the NHDPlus dataset and prepared for use with SSNs (Nagel et al. 2015). The observed water temperature data were queried from the NorWeST database, which consists of temperature logger data collected by numerous agencies and groups and contains over 220,000,000 observations at greater than 22,700 sites throughout the western United States (Isaak et al. 2017). Observed temperature sites that had multiple observations within a day and observations on at least 90% of days within a month were averaged in order to obtain a monthly mean water temperature value which was used within the model. The model fits nine spatial covariates and two temporal covariates. The spatial covariates are elevation (m), canopy (%), slope (m/m), annual precipitation (mm), cumulative drainage area (km²), northing coordinate (km), upstream watershed area that is lake or reservoir (%), the amount of flow that is base flow (%), and tailwater (binary - 0, 1). The majority of these covariates are from NHDPlus, with the exception of base-flow index (developed by Wolock 2003) and northing coordinate and tailwater (determined by Isaak et al. 2017). Each of these covariates was calculated at a 1 km interval, and GIS was used to spatially link these covariates with the stream network. The

temporal covariates are air temperature (degrees Celsius) and flow (m³/s). Air temperature was obtained from the NCEP RegCM3 reanalysis in the form of 15 km gridded data (Hostetler et al. 2011). The data were subset to include only grid cells within the spatial extent being modeled. Monthly mean air temperature values were calculated, and these values were linked to water temperature observations by year. Flow time series were queried from the USGS National Water Information System for gages within the spatial extent being modeled. Gaps in the time series were filled using an iterative PCA approach (Josse and Husson 2016). Monthly means were calculated, and these values were linked to water temperature observations by year.

The data were split into a training dataset and a testing dataset, such that approximately 80% of the data were used for model fitting and 20% of the data were used for model validation. When a site had data in multiple years, all data for that site were included in either the training or testing dataset rather than being split between them. Leave-one-out cross validation was also performed on the training dataset, and three metrics were calculated on each the training dataset and the testing dataset to quantify the performance of the model: the square of the correlation coefficient between observations and predictions (r^2), the root mean square prediction error (RMSPE), and the mean absolute prediction error (MAPE). The model fits were used to predict water temperature values at a 1 km resolution for all rivers in the modeled region for the period 2002-2011 using the universal kriging equation which accounts for both the model predictors and spatial autocorrelation (Cressie 1993). The years we analyze represent the 1993-2011 scenario used in the original NorWest model (Isaak et al. 2017).

Analyses – spatial and temporal patterns of salmonid thermal exposure

Monthly mean stream temperatures were extracted for each distribution point in ArcMap. Occurrences that snapped > 500m to a stream were removed. For holding and incubation, we analyzed stream temperature during the peak of that life stage. Due to differences in juvenile rearing strategy, we examined stream temperature in the first month following peak emergence. Populations with fewer than 100 occurrences (see Fig. 1) were not examined. Thermal exposures of populations were compared using density plots and analyses of variance (ANOVAs); each life stage was compared separately. All analyses were completed in R.

RESULTS

Stream temperature

Analyses were completed for the regions of central California and Mid-Columbia; note that these names do not correspond to Chinook population names. Data is currently unavailable (as of 15 July 2018) for two regions with anadromous salmonids, the Clearwater and Salmon regions. The remaining regions are in queue to run on our computing core (Fig. 2).

Preliminary SSN models for the central California region had a high degree of predictive capability in all months. The leave-one-out cross validation resulted in r^2 values of 0.86 – 0.96, RMSE values of 0.70 – 1.71, and MAPE values of 0.50 – 1.19 for the central California region. For the Mid-Columbia region, the r^2 values were 0.79 – 0.94, RMSE values were 0.67 – 1.71, and MAPE values were 0.45 – 0.81. The out-of-sample validation also showed predictive capability of the models, with r^2 values of 0.70 – 0.86, RMSE values of 1.18 – 2.84, and MAPE values of 0.85 – 2.27 for the central California region; and r^2 values of 0.48 – 0.88, RMSE values of 0.90 – 2.15, and MAPE values of 0.65 – 1.17 for the mid-Columbia region (Table 1, Fig. 3).

There were clear trends in the covariate effects on water temperature in central California (Fig. 4). Elevation had a strong negative (cooling) effect in all months; precipitation had a negative effect in most months; air temperature had a positive (warming) effect in most months; tailwater had a negative effect in the spring, summer, and fall (April – September) and a positive effect during the winter (November – January); flow had a negative effect in the spring and summer (March – September); and riparian canopy had a negative effect in the summer and fall (June – October). The predicted temperature values for all rivers were mapped (central California temperatures in April and October shown in Fig. 5) and were utilized in statistical analyses examining the thermal regimes of Chinook populations and life stages.

Patterns in thermal exposure

Considerable phenological variation exists within and between populations (Appendix 1 Table S1.1). For example, peak spawning for spring run populations occurs August-October, September-October for summer, and October-December for fall runs. There is not a clear latitudinal cline in peak spawning month, and several Pacific Northwest populations spawn in the same month as Central Valley populations. The only winter run population spawns in May along the Sacramento River.

Populations were exposed to temperatures ranging from near freezing (e.g. holding Snake River fall-run) to above 20 C (holding Central Valley and Mid-Columbia River spring-runs) (Table 2, Fig. 6). In general, Central Valley populations (both fall- and spring-runs) experienced significantly warmer and narrow temperature regimes for each life stage compared to other populations. This is particularly true for Central Valley fall-run during holding and incubation. Central Valley spring-run were exposed to fairly warm temperatures during peak holding in June (14.86±2.70 C), but Mid-Columbia spring-run holding in June and July were exposed to even warmer temperatures (15.16±3.65 C). The warmest occurrences from the Central Valley occurred along the Feather River. The John Day River system from the Mid-Columbia had the warmest temperatures for spring-run during peak holding.

Within the Central Valley, fall, spring, and winter-runs were exposed to unique thermal regimes during each life stage (Table 2). Spring-run were exposed to the warmest temperatures during peak holding, but the Sacramento River winter-run peak incubation occurs in temperatures about 7 C warmer from the next highest temperatures experienced by other populations during peak incubation. This population also was exposed to temperatures during early rearing that were 4.9-14.6 C warmer than other populations during early rearing.

Only 9 out of 108 possible population pairs experienced similar thermal regimes during at least one life stage (Table 2, Fig. 6). Most of the similarities stemmed from geographic proximity and identical or adjacent month of life stage (e.g. Lower Columbia River and Deschutes River fall-runs both have peak incubation in December and are in similar geographic locations). However, some spring runs were similar to fall runs despite having dissimilar life stage months. For example, Deschutes River and Snake River fall runs both arrive in November whereas peak holding for Lower Columbia River spring-run occurs in May, but all three populations experienced similar temperatures during peak holding. Our analyses indicate that the stream temperature results predicted similar temperature regimes for late spring (~May) and late autumn (~November) in the Columbia/Snake/Deschutes River basin. The fall-runs, however, as less likely to be negatively impacted by warm temperature as they spawn very soon after arrival

whereas spring-run populations will hold in the warmer summer waters for months prior to spawning (see Section 2).

DISCUSSION

Stream temperature model

The spatial stream temperature network model we employed has been shown to be an effective predictor of stream temperatures throughout the western U.S. for August (Isaak et al. 2017). We expanded this model to all months of the year for watersheds in the western U.S. hosting anadromous salmonids. Our expanded model had high predictive power (minimum testing dataset $r^2 = 0.64$, average ~ 0.8). Temperature error was moderate (~ 1 C; Table 1), suggesting some caution when interpreting results near survival thresholds.

Temperature is the principal abiotic factor that influences a population's evolutionary trajectory (Brannon et al. 2004), and this is especially true for aquatic ectotherms that are dependent on their external environment. Still, the number of large-scale aquatic studies is dwarfed by the abundance of terrestrial studies (Parmesan 2006), with the primary limitation being the previous lack of accessible environmental layers. Our stream temperature model paves the way for large-scale aquatic studies in western U.S. These stream temperatures can be used to examine temperature exposure across populations (as we did for Chinook salmon), explore potentially suitable thermal habitat (e.g. for reintroductions), or predict stream temperature changes based on future air temperature and precipitation predictions, making our work particularly important in the era of rapid anthropogenic change.

Thermal exposures of Chinook populations

We used our monthly stream temperature predictions to assess patterns in temperature exposure across populations. Specifically, we aimed to calculate if California salmonid populations inhabit a distinct temperature regime compared to Pacific Northwest populations. We found that most populations, including those in California, are exposed to significantly different temperatures during peak holding, incubation, and early juvenile rearing.

We also found distinctions between runs within the Central Valley. In the Central Valley, winter-run and spring-run Chinook are declining more rapidly than fall-run. Winter- and spring-runs experience high temperatures compared to fall-run (especially during holding for spring-run and incubation for winter-run). High temperature exposure during critical life stages may be contributing to their decline. A broader comparison among other populations throughout the Western U.S. will better elucidate these patterns.

Some populations are exposed to temperatures greater than recommended by the EPA Region 10 thermal criteria for salmonids (U.S. EPA 2003). Holding spring-run adults in the Feather River (Central Valley) and the John Day River system (Mid-Columbia) can experience temperatures greater than 20C (Torgersen et al. 1999); the recommended maximum temperature for holding adults is 16C, although the recommended threshold for migrating adults is 20C. Peak incubation for Sacramento River winter-run often exceeded the recommended threshold of 13C (U.S. EPA 2003). These results highlight that some populations – even those that are managed – are exposed to temperatures near or above the recommended thresholds during certain life stages. For spring-run and winter-run, much of their former spawning, incubation, and rearing habitat is

now inaccessible, and these populations are now exposed to warmer temperatures than historically, perhaps contributing to their decline.

Limitations in our approach

Our stream temperature model allows a thorough comparison of temperature exposure during different salmonid life stages for multiple populations simultaneously. Prior to our work, analyses utilizing stream temperature focused on a few populations or rivers. Isaak et al. (2017) allowed for a comparison of temperature exposure during August. A broad-scale comparison across multiple regions, however, does have some limitations.

The occurrence dataset assumes that fish are found in the temperature predicted by the model, but the spatial resolution of SSN model (1km) may not have high enough resolution to depict microreaches with more suitable temperatures. It is well-documented that freshwater fish may behaviorally thermoregulate by moving to microhabitats within the stream (Bardach and Bjorklund 1957, Kaya et al. 1977, Berman and Quinn 1991, Headrick and Carline 1993, Fullerton et al. 2017). For example, although we found that some Mid-Columbia spring-run in the John Day River system were holding in temperatures above 20C, a study found that spring-run held in small pools significantly cooler than the surrounding river temperature (Toergersen et al. 1999). Further, a comparison of the NorWest mean August stream temperature model (spatial resolution of 1km) to airborne thermal infrared remote sensing (continuously sampled) found that lower spatial resolutions (> 1 km) predicted fewer and more distantly-spaced low-temperature patches compared to higher resolutions despite the fact that the datasets were similar (Fullerton et al. (2017).

Our spatial resolution (1km) may not predict the temperatures of small thermal refugia, potentially overestimating the temperatures salmonid populations are exposed to. Higher resolutions, however, are currently only feasible for focused or small-region studies (i.e. a few small watersheds or streams) and untenable for large regions (i.e. all streams/rivers in western North America). Further, high resolution data often stems from a narrow time range (e.g. a few days of a month in a single year; see Fullerton et al. 2017) whereas range-wide models can predict monthly or even daily temperatures for multiple years. Further, these thermal refugia are often patchy (e.g. Torgensen et al. 1999, Fullerton et al. 2017), indicating that salmon will be exposed the warmer stream temperatures at some point as they move among thermal refugia.

Subsurface flow may result in cooler temperatures at the bottoms of rivers or in large pools, which our SSN model may not indicate. Fine-scale temporal movements of fish may result in different temperature exposures. For example, juvenile sockeye salmon show a dial migration pattern in stratified water columns, possibly to avoid debilitating high temperatures (Brett 1971). However, we assume that the rivers in our dataset are not stratified like lakes.

The SSN model predicts mean monthly stream temperature at every river kilometer in the western U.S., and our phenology database depicts the peak month of each life stage for each population. Mean monthly temperature, however, may hide daily minimum or maximum temperatures beyond the threshold of survival. The Region 10 temperature criteria used a 7DADM (7 day average daily maximum) to derive thermal criteria for salmonid populations in Oregon, Washington, Idaho, and Alaska (U.S. EPA 2003). This value is appropriate for stream-specific sites with lots of temperature data, but would be computationally too expensive for the spatial scope analyzed here.

The salmon phenological and spatial analyses rely heavily on the quality and accuracy of our occurrence dataset. To align with the SSN model, the dataset is based on modern occurrences after 1993, which is after the anthropogenic disruption of habitats by dams and destruction resulted in distributional changes and population losses. Ideally, distribution modeling should be based on pre-anthropogenic disruption in order to understand the environmental requirements of a species (Agrawal et al. 2005, FitzGerald et al. 2018). Because our dataset is post-disruption, we cannot currently determine if our results reflect population-specific temperature optima or the best conditions currently available to each population.

PART 1: FIGURES AND TABLES

Key	ESU	Run	N
	California Coastal	Fall	1252
	Central Valley	Fall	1087
	Deschutes River	Fall	1267
	Lower Columbia River	Fall	2495
	Oregon Coast	Fall	5553
	Puget Sound	Fall	7634
	Snake River	Fall	1193
	S. Oregon N. California Coast	Fall	1154
	Upper Klamath Trinity Rivers	Fall	2791
	Upper Columbia River	Fall	50
	Washington Coast	Fall	2932
	Central Valley	Spring	681
	Lower Columbia River	Spring	790
	Mid Columbia River	Spring	4160
	Oregon Coast	Spring	512
	Puget Sound	Spring	2770
	Snake River	Spring	4873
	S. Oregon N. California Coast	Spring	96
	Upper Klamath Trinity Rivers	Spring	1608
	Upper Columbia River	Spring	882
	Upper Willamette River	Spring	1871
	Washington Coast	Spring	1398
	Sacramento River	Winter	187
	Puget Sound	Summer	1531
	Snake River	Summer	1813
	Upper Columbia River	Summer	770
	Washington Coast	Summer	911

Figure 1. Occurrences for each defined population, separated by A) fall runs, B) spring runs, and C) summer runs and the single winter run. D) shows the legend and number of occurrences for each population. Note that we do not have occurrences for California Coast spring-run – which are mostly extinct – late-fall runs – which are not well-studied – or Deschutes River summer-run.
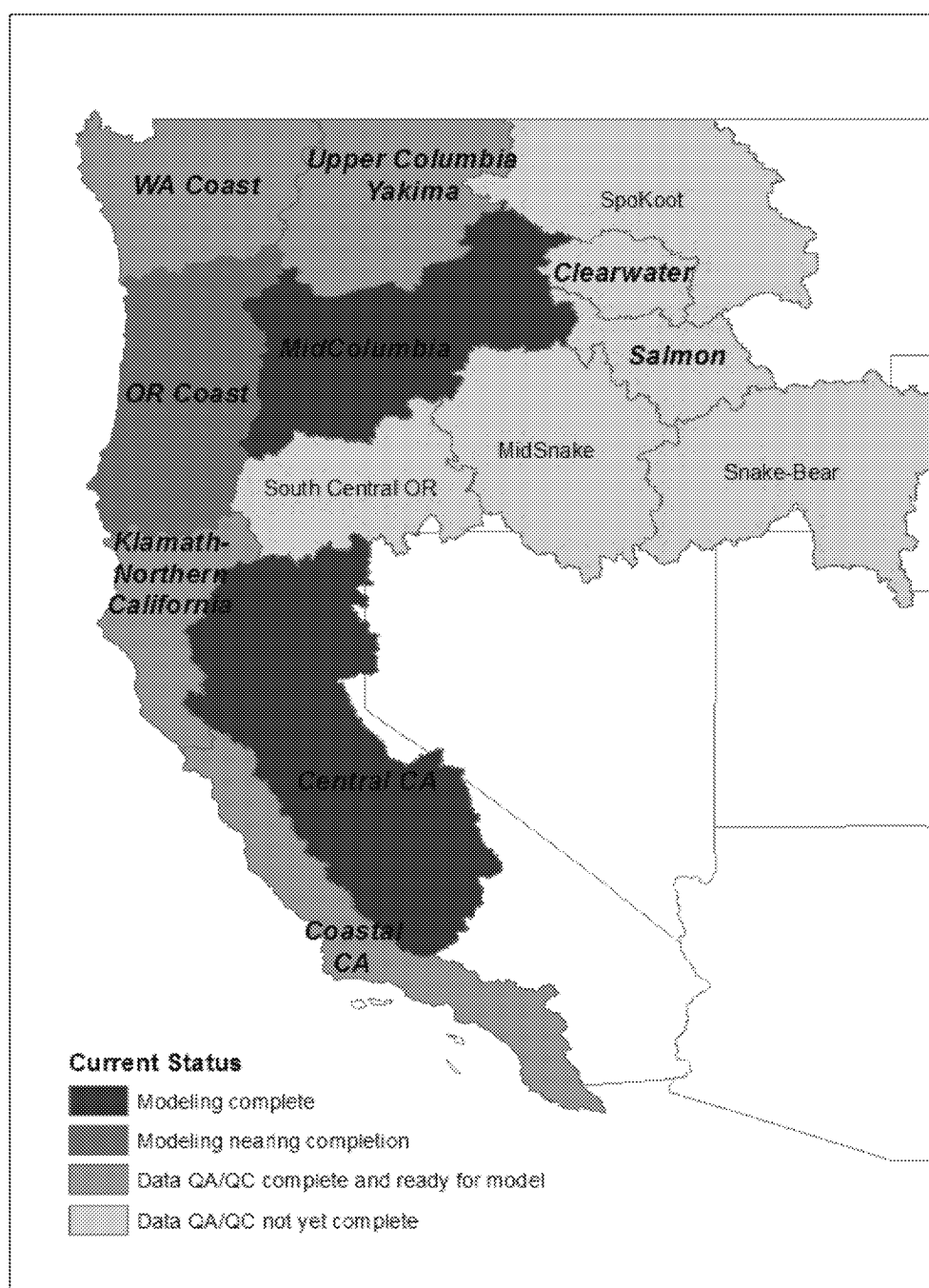
Figure 2. Status of stream temperature modeling project. Modeling has been completed for two regions.[2] Data is currently unavailable for six regions, but note that only the Clearwater and Salmon regions (bolded) are important for anadromous salmonids.

---

[2] Modeling was completed for the Coastal CA, Klamath-Northern California, and WA Coast regions by January 31, 2019, but we did not have time to incorporate those results into this Draft.

Table 1. Number of temperature observations (T_w n), predicted r^2, root mean square prediction error (RMSE) and mean absolute prediction error (MAPE) for each month (1993-2011) for the training dataset (in-sample) and testing dataset (out-of-sample) for the SSN model of: a) central California region, and b) Mid-Columbia region.

A)

Month	In-sample				Out-of-sample			
	T_w n	r^2	RMSE	MAPE	T_w n	r^2	RMSE	MAPE
January	1158	0.93	0.85	0.53	278	0.81	1.22	0.85
February	1171	0.95	0.79	0.50	289	0.86	1.18	0.87
March	1178	0.95	0.92	0.62	291	0.86	1.45	1.17
April	1212	0.94	1.00	0.69	295	0.83	1.75	1.44
May	1282	0.90	1.33	0.94	323	0.78	2.12	1.70
June	1645	0.86	1.71	1.19	406	0.76	2.42	1.89
July	2087	0.87	1.69	1.11	515	0.70	2.84	2.27
August	2295	0.90	1.41	0.92	570	0.75	2.54	1.97
September	2014	0.93	1.12	0.74	501	0.81	1.93	1.48
October	1458	0.95	0.86	0.59	360	0.82	1.40	0.97
November	1202	0.96	0.70	0.48	297	0.82	1.28	0.97
December	1141	0.95	0.82	0.59	284	0.74	1.50	1.09
Average	1487	0.92	1.10	0.74	367	0.80	1.80	1.39

B)

Month	In-sample				Out-of-sample			
	T_w n	r^2	RMSE	MAPE	T_w n	r^2	RMSE	MAPE
January	974	0.86	0.69	0.49	245	0.68	1.00	0.71
February	997	0.89	0.63	0.45	249	0.71	0.88	0.60
March	995	0.91	0.62	0.45	248	0.80	0.89	0.63
April	1078	0.94	0.63	0.43	271	0.85	1.06	0.69
May	1724	0.92	0.86	0.62	431	0.85	1.26	0.91
June	3633	0.91	1.02	0.74	908	0.85	1.36	1.02
July	6378	0.93	1.00	0.68	1601	0.82	1.60	1.11
August	7435	0.94	0.88	0.58	1852	0.81	1.51	1.04
September	5522	0.96	0.70	0.46	1381	0.84	1.14	0.79
October	2229	0.95	0.68	0.44	557	0.89	0.99	0.69
November	1242	0.93	0.78	0.53	311	0.79	1.19	0.89
December	1065	0.88	0.76	0.52	272	0.64	1.32	0.84
Average	2773	0.92	0.77	0.53	694	0.79	1.18	0.83

A

B

C

D
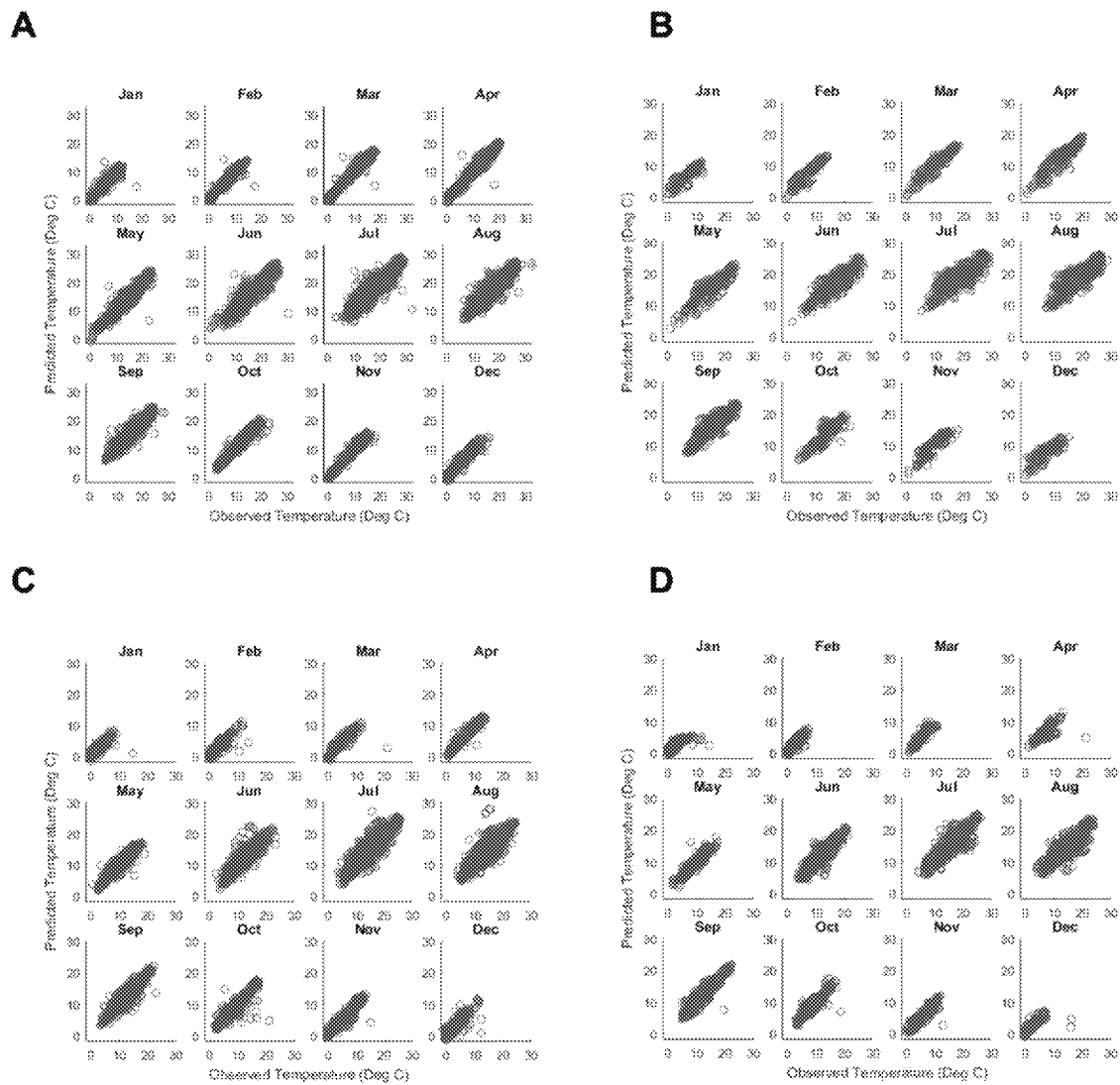
Figure 3. Observed and predicted water temperature values for 1993-2011 for: A) Central California training data, B) Central California testing data, C) Mid-Columbia training data, and D) Mid-Columbia testing data.
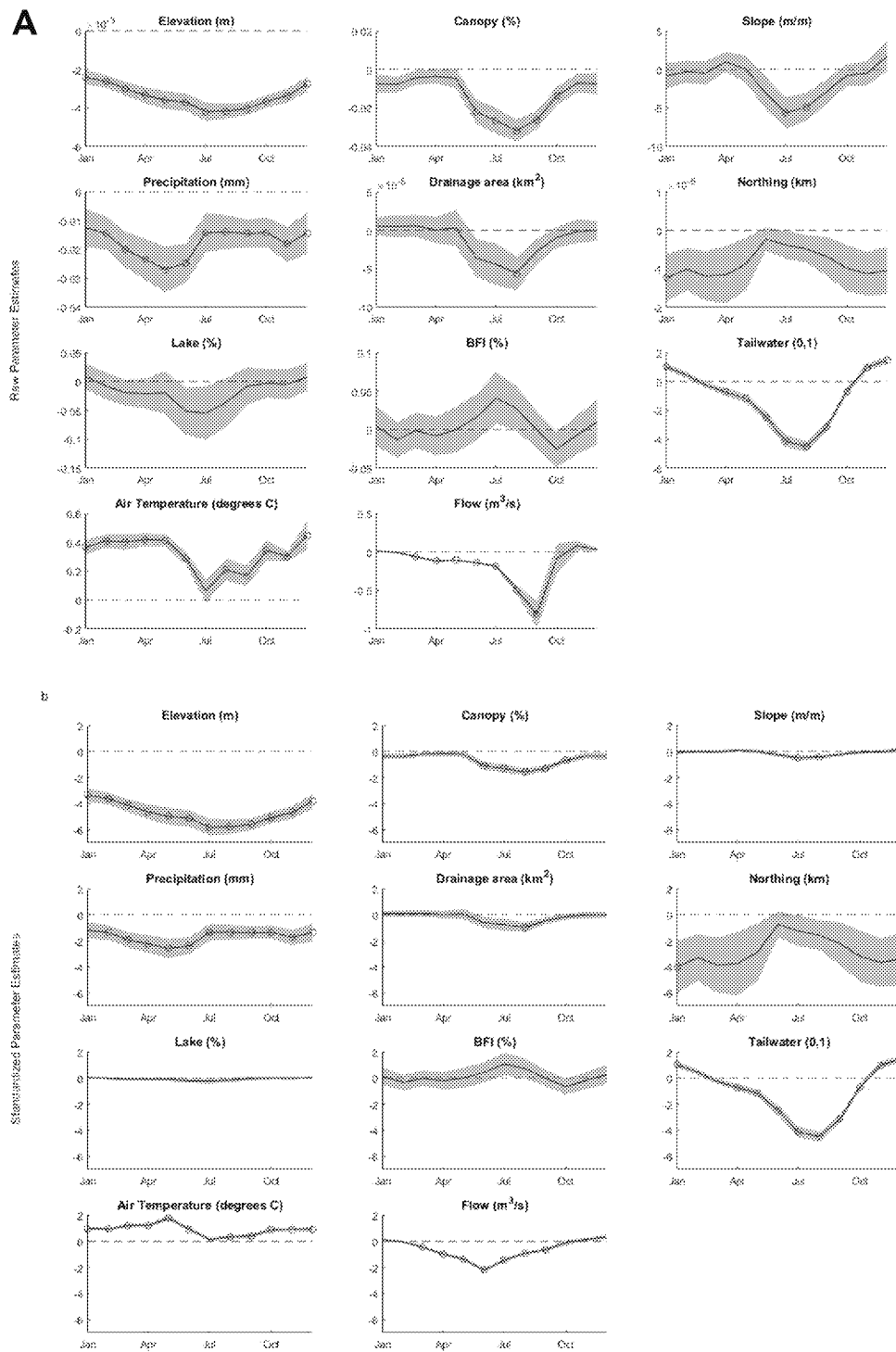
Figure 4. Raw parameter estimates (A), and standardized parameter estimates (B) for all model covariates in all months. Solid line shows the parameter estimate and shaded region shows +/- 1 standard error. Red circles indicate covariates that had a significant effect (p < 0.05).
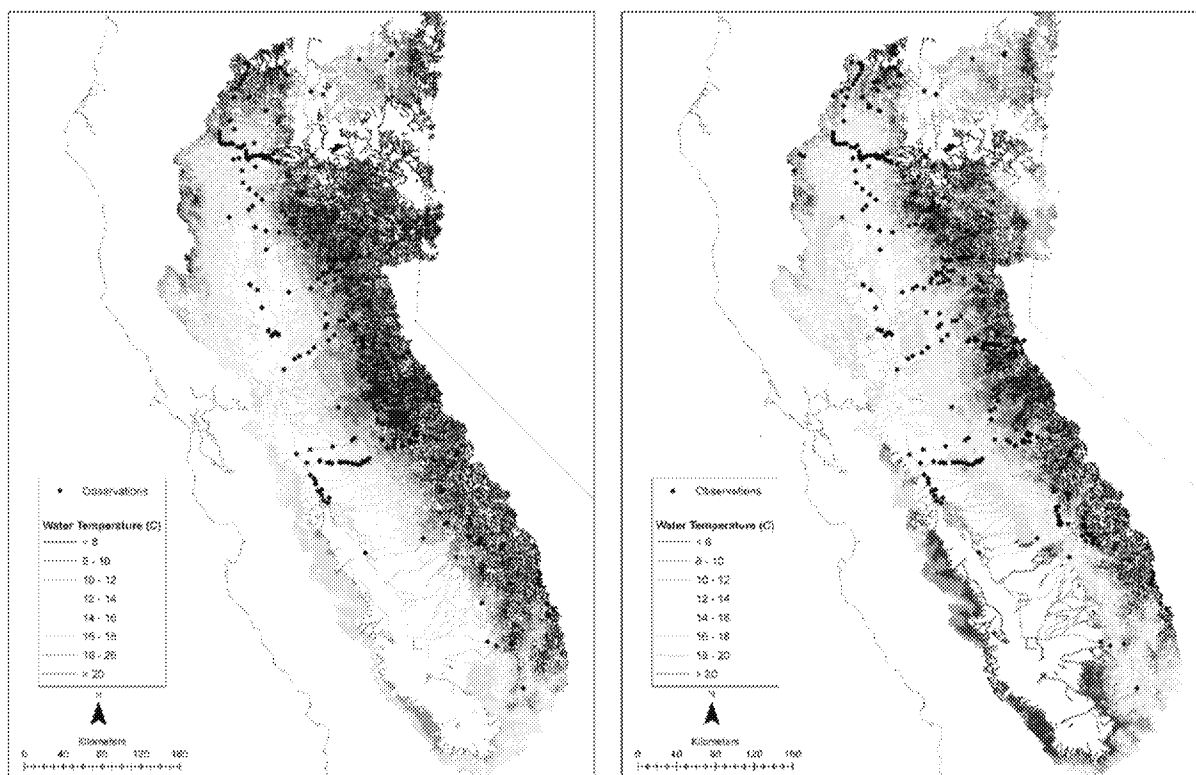
Figure 5. Preliminary predicted water temperature values and empirical stream temperature observations (black dots) for the central California region for 1993-2011 for April (left) and October (right).
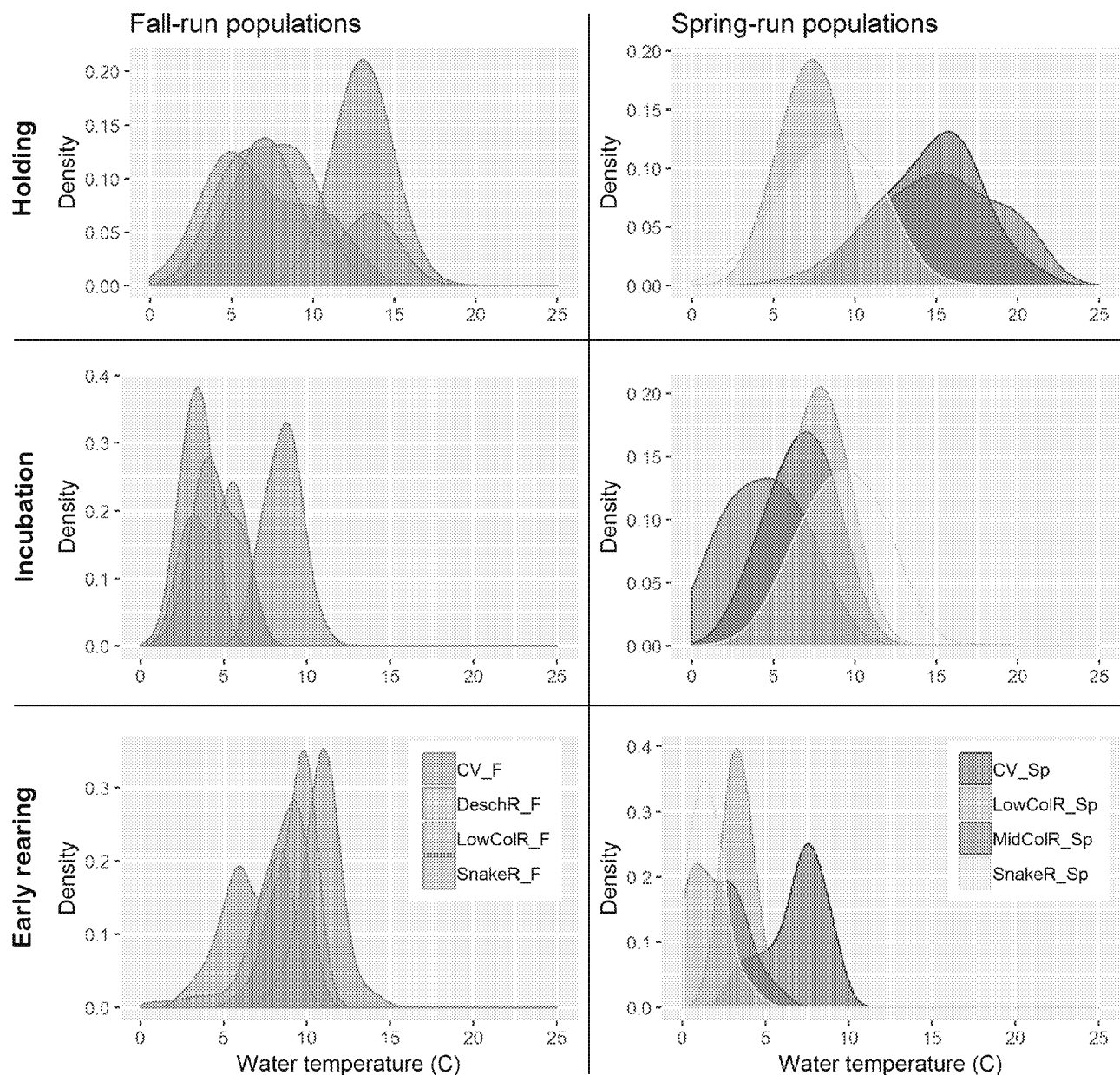
Figure 6. Comparison of the thermal exposures of Chinook during peak holding, peak incubation, and early rearing in the Central California and mid-Columbia regions for fall-run (left panel) and spring-run (right panel) populations. The populations are Central Valley (fall and spring), Deschutes River (fall), Lower Columbia River (fall and spring), Mid-Columbia River (spring), Snake River (fall and spring).

Table 2. Summary statistics for temperature exposure during peak holding, peak incubation, and early rearing for Chinook populations (run shown in parentheses). Mean, SD, Min, and Max refer to temperature values (°C). Population/life stage groupings with identical superscript letters (shown next to mean) are not significantly different (Tukey's HSD test; $P > 0.05$); no superscript indicates that population is significantly different from all others.

Population	HOLDING				INCUBATION				REARING			
	Mean	SD	Max	Min	Mean	SD	Max	Min	Mean	SD	Max	Min
Central Valley (fall)	13.06	0.85	15.79	10.96	8.56	0.93	11.09	6.44	10.88	1.06	14.33	7.78
Deschutes River (fall)	7.17[a]	1.96	11.60	3.83	4.51[d]	1.38	6.99	2.05	9.23	1.04	10.52	5.67
Lower Columbia River (fall)	8.84[b]	3.19	13.97	4.50	4.54[d]	1.19	6.35	1.82	6.80[e]	1.68	9.30	2.82
Snake River (fall)	6.81[a]	2.86	11.42	0.24	3.31	0.68	5.58	1.11	8.21	1.75	10.23	0.55
Central Valley (spring)	14.86[c]	2.70	20.59	9.44	6.64	1.69	9.45	3.08	6.83[e]	1.72	9.44	2.81
Lower Columbia River (spring)	7.24[a]	1.38	11.39	4.31	7.88	1.32	16.39	5.72	3.33	0.69	6.25	1.82
Mid Columbia River (spring)	15.16[c]	3.65	21.81	4.54	4.41[d]	2.24	11.78	0.03	2.10	1.53	6.80	0.00
Snake River (spring)	8.43[b]	2.70	15.22	0.83	9.19	2.25	17.21	2.92	1.18	1.10	5.24	0.01
Sacramento River (winter)	10.11	0.38	10.65	9.07	16.12	1.30	22.87	13.96	15.78	0.69	18.92	14.61

Part 2. Can we improve site-specific temperature management in the Central Valley by using thermal performance curves?

INTRODUCTION

Region 10 criteria provide binary temperature thresholds that managers need to meet in order to protect salmonids, but most of the research involved in setting these thresholds was based on Pacific Northwest populations. In California, water temperature often meets or exceeds these thresholds, especially during years of extreme temperature or drought. For example, in 1977 in the second of two subsequent drought years, water temperatures in the Sacramento River exceeded the requirements of every life stage from July through October (Boles 1988). A 4-year drought from 2012-2016 resulted in high egg mortality of winter- and fall-run when temperatures in the Sacramento River exceeded 16°C (Bland 2015), above the Region 10 threshold 13°C for spawning (U.S. EPA 2003). In instances when temperature requirements cannot be met, the Region 10 binary thresholds do not provide guidance on how cold water resources should be best be managed to minimize negative impacts on salmonid populations. Although there is currently not enough information to assess if new temperature thresholds for California salmonids are needed (Zillig et al. in prep), here we develop a framework using continuous thermal performance curves (TPCs) to quantify thermal effects across life-stages and ultimately help prioritize cold water resources in years when Region 10 criteria cannot be met.

Thermal performance curves quantify the relationship between temperature and performance of a particular process (e.g. survival, growth, reproduction). Laboratory experiments take a direct, explicit approach to quantifying the thermal effects on a trait in a controlled setting by varying a single variable, i.e. temperature, while keeping all other variables (e.g. flow, photoperiod) constant. Modeling the effects of temperature on physiological performance results in a thermal performance curve (TPC) that describes temperature-dependent effects on a trait (Schulte et al. 2011). For example, by relating juvenile growth from 11 Chinook populations to temperature, Perry et al. (2015) defined a TPC that calculates how temperature affects juvenile growth (Fig. 8). TPCs thus define the optimum temperature (the temperature at which performance is maximized) as well as how deviations from the Region 10 thresholds affect performance. If the shape of the TPCs differs substantially among life-stages, then exceeding Region 10 criteria by the same amount can lead to substantially different population impacts. TPCs are therefore ideal to compare temperature-dependent responses across life stages, between populations, and to changing temperatures (Eliason et al. 2011, Zillig et al. in prep).

Our framework provides a quantitative approach for assessing thermal impacts in Central Valley rivers across runs and life stages, illustrated in Fig. 9. Specifically, we examine thermal effects on energy use for adults holding, egg-to-fry survival, and juvenile growth rate using the best temperature-dependent models currently available for Chinook. These TPC models are combined with local distribution and phenology data and stream temperature to translate spatial-temporal temperature data into maps of life stage-specific performance in space and time. Thermal performances across life stages are then compared in a spatial-temporal context to determine which life stages along a river are the most vulnerable to temperatures exceeding the Region 10 thresholds. In years when the Region 10 criteria cannot be met, this method provides local managers the information to appropriately prioritize cold water resources to minimize the negative thermal impacts on salmonid populations.

METHODS

Overview of framework

To assess thermal impacts across life stages in different rivers, we need 1) local phenological and spatial data to determine when and where different life stages occur, and 2) water temperature along that river. These temperatures are used as inputs in various stage-specific thermal performance models that relate temperature to physiological performance (Fig. 1). The models that we employ are based on the best data currently available for Chinook, but can be updated or changed as better data become available. To help elucidate which life stages are the most vulnerable to negative thermal impacts, thermal effects are compared between life stages via conversion to a common currency, percent effect. Below, we describe in detail how each of the components of this approach (local spatial and phenological datasets, temperature monitoring data, and thermal performance models) are combined to estimate thermal impacts along a river.

Site-specific phenology and spatial locations

Stream selection

Taking into consideration the availability of temperature data, Chinook run timing, and the availability of phenological and spatial data, we illustrate our thermal performance curve modeling framework on Clear Creek, Stanislaus River, and Tuolumne River. These streams cover a breadth of run scenarios, amount of available habitat (measured in river km), and flows (Table 1). Clear Creek has both fall and spring runs, whereas the Stanislaus and Tuolumne Rivers currently only have fall run because spring run have been extirpated. These streams also represent different amounts of available habitat for salmon: less than 50 km for Clear Creek, and 50-100 km for Stanislaus and Tuolumne Rivers. Clear Creek has a low mean annual flow, Stanislaus has a moderate flow, and the Tuolumne has the highest flow. Finally, these streams are all regulated by hydroelectric dams, allowing for a controllable response based on scientific information.

Distribution models of phenology and spatial locations

We obtained phenological and spatial data from published sources, technical reports, and/or raw data for each life stage per stream (Table 1). We fit a daily phenological distribution model based on Julian day and count (e.g. number of live fish or redds) for each life stage along each river (Table 2, Supp. 1). Similarly, we fit a spatial distribution model based on count per river km (Table 3, Supp. 1B). We calculated summary statistics and then sampled from the fitted distributions for use in thermal performance models. Unless otherwise state, Gaussian (normal) models were fit.

Water temperature

Observed mean daily temperatures were extracted from the temperature monitors used in the NorWest project (downloaded from https://www.fs.fed.us/rm/boise/AWAE/projects/NorWeST/StreamTemperatureDataSummaries.shtml) using ArcMap. To obtain daily stream temperatures for all river kilometers, we linearly

interpolated actual stream temperature observations to create stream temperatures along a river that matched the spatial/temporal resolution of the spatial and phenological data (i.e. 1km/daily). Gaps of less than 30 days were filled in for all monitors before interpolating. In the rare instance where more than one temperature recording was present per river kilometer for a specific date, we took the average. We have Clear Creek temperatures for 2002-2015, Stanislaus River temperatures for 1993-2014, and Tuolumne River temperatures for 1993-2014, but illustrate our models using temperatures for 2013 (Fig. 2).

Models
Temperature-dependent metabolic expenditure and spawning success

Sexually immature spring-run chinook adults migrate toward the spawning grounds a few months before spawning is initiated, holding in low-flow pools as their gonads mature and stream temperatures drop (Moyle 2002). During this period, they do not eat McCullough 1999) and therefore have a finite amount of energy to cover the costs of maintenance metabolism. Energy use increases exponentially with temperature, so here we employ a temperature-dependent metabolic expenditure model to calculate the energy expended by an adult holding prior to spawning (from Martin et al. 2015):

$$B_{h\,i} = c_0 M^b e^{DT}$$

where $B_{h\,i}$ is the maintenance metabolism, or how much energy is used by an adult salmon at a given temperature per unit time. Values for b (-0.217 [unitless]), the mass exponent of maintenance, and D (0.068 [unitless]), the temperature exponent of maintenance, were originally parameterized by Rao (1968) on rainbow trout and were adapted to Chinook in Lake Michigan by Stewart (1980). The c_0 value was parameterized using Chinook data (Martin et al. 2015) and converted to reflect our analyses on a daily time scale (1572.24 mgO_2 d^{-1} kg^{-1}). The mass, M, was estimated at 7.37 kg based on the relationship between fork length (L_F) and somatic and gonadal masses at the start of migration (average female L_F = 815 mm; Bowerman et al. 2017), but M can be easily catered to a specific river. Temperature (C°) is value T in space and time, obtained from linear interpolations of observed stream temperatures. After running the model to calculate the maintenance metabolism at a single location in space and time, we summed daily energetic expenditures across time to determine the total energy used per unit mass by an adult holding for n time steps (here, days) at a given location:

$$E_{hTOT} = \sum_{i=1}^{n} B_{h\,i} t$$

where n is the number of days holding and t represents the time step, in our example, 1 day. Salmon arriving after peak spawning were assumed to spawn immediately and have no holding costs. We began running our model from the earliest arrival day for each river minus a 30 day buffer; for example, the earliest arrival day on Clear Creek was Julian day 83 (~March 25) so we began running our model from Julian day 53 (~February 23). Similarly, we included a 30 day

buffer after the last reported spawning date. These buffers allow us to estimate holding costs for early arrivals and late spawners that may be missing from our dataset due to low abundance, lack of sampling, or inability to distinguish from other runs.

The length of the holding period, n, was determined by the differential between day of arrival and spawning date. However, little information exists to calculate the exact length of holding for a fish; for example, we don't know if early arrivals with a long holding spawn earlier than late arrivals. To calculate n for a given arrival date, we randomly sampled spawning date from the phenological distribution 1,000 times, running the model each time. Results were averaged over the 1000 replicates and converted from mgO_2 kg^{-1} to MJ kg^{-1} (1 mgO_2 = $1.358442*10^{-5}$ MJ; see Martin et al. 2015).

Adult salmon do not consume food during migration or spawning, and therefore have a finite amount of energy once migration commences to reach the spawning grounds, hold until proper spawning conditions, form gonads, and spawn. Post-spawning, salmon carcasses have ~4 MJ kg^{-1} of energy (E_D), indicating that this energy is unavailable for migration or reproduction costs (Crossin et al. 2004, Bowerman et al. 2017a, Plumb 2017). Therefore, in order to successfully spawn, energy expenditure must not exceed E_D:

$$E_I - (E_M + E_H + E_G) \leq E_D$$

where E_I is the energy at the start of migration, E_M is energy used during migration, E_H is energy used during holding, and E_G is energy allocated to gonad formation. These parameters can differ to some degree both within and among populations (Crossin et al. 2004, Bowerman et al. 2017a), so we assumed a variable starting muscle energy density (spring-run: E_I = 11.7 ± 1.0 MJ kg^{-1}, Bowerman et al. 2017; fall-run: 8.0 ± 1.0 MJ kg^{-1}, Martin et al. 2015). Migration costs depend on the migratory difficulty, i.e. distance travelled, elevation, speed, temperature, and flow (Crossin et al. 2004, Mesa and Magie 2006, Martin et al. 2015, Bowerman et al. 2017). For adults migrating up the Sacramento River to spawn in Clear Creek, we estimated an energy expenditure of E_M =2.5 MJ kg^{-1} for spring-run and E_M =2.0 MJ kg^{-1} for fall-run Chinook (Martin et al. 2015). Our temperature-dependent metabolic expenditure model calculates holding costs (E_H; see above). Gonad formation (E_G) costs 14% of starting somatic energy density (Bowerman et al. 2017), and we assumed that a similar percentage is allocated from muscle. Postspawned females died with 3.4 MJ kg^{-1}, providing an estimate for E_D (Bowerman et al. 2017). We use values for muscle energy density because muscle energy stores – but not skin or viscera energy density – decline with migratory difficulty (Mesa and Magie 2006, Bowerman et al. 2017).

We randomly sampled from the E_I distribution 1,000 times and ran the above model for each spatial/temporal pixel to calculate the percent likelihood that an individual would have enough energy to successfully spawn (i.e. energy used is $\leq E_D$).

Temperature-dependent embryonic mortality

In the Central Valley, embryos incubate for ~2-4 months prior to emergence (Boles 1988), and survival through the embryonic stage is strongly dependent on temperature (McCullough 1999). We therefore apply a temperature-dependent embryo mortality model based on daily incubation temperatures to calculate the percent mortality of eggs spawned at a given location in space and time (Martin et al. 2017):

$$M_T = 1 - \prod_{i=1}^{n} \exp\left(-s_T(T_i - T_{crit})\right)$$

where M_T is the temperature-dependent mortality throughout the embryonic period, s_T is a parameter defining the slope at which the mortality rate increases with temperature above T_{crit}, T_{crit} is the temperature below which there is no mortality due to temperature, and Ti is the temperature experienced at the ith day of development. The model was parameterized with winter-run Chinook field observations of egg-to-fry survival data, resulting in $T_{crit} = 12.0$ °C and $s_T = 0.024$ °C^{-1}d^{-1} (Martin et al. 2017).

The time required for eggs to hatch is temperature-dependent (Boles 1988). To determine the length of the embryonic period, n, at each spatial-temporal location, we implemented the temperature-dependent maturation function by Zueg et al. (2012):

$$1 \leq \sum_{i=1}^{n} 0.001044\,C^{-1}\,d^{-1} \times T_i + 0.00056\,d^{-1}$$

where emergence occurs when the sum reaches 1. The temperature-dependent embryo mortality model was then run using the calculated embryonic period for each spatial-temporal location. Finally, we converted the mortality proportion into percent survival.

Temperature-dependent juvenile growth rate

The ability to successfully smolt is size- and temperature-dependent (Ewing et al. 1979, Healey 1991, McCullough 1999), such that fish with low growth rates may undergo desmoltification, revert to parr, and return to freshwater, resulting in subsequent high juvenile mortality (McCullough 1999). Growth rates of fish are temperature-dependent, and so we apply a juvenile growth model based on temperature (Perry et al. 2015):

$$\Omega = Food * d * (T + T_{corr} - TL) * (1 - \exp(g * (T + T_{corr} - TU)))$$

where Ω is the mass-standardized growth rate (specific growth rate per 1g of fish), T is mean temperature over the growth period, d and g are shape parameters, and T_L and T_U are parameters defining the lower and upper thermal limits at which the growth rate is zero. Perry et al. (2015) parameterized the model with experimental juvenile growth data from multiple Chinook populations, resulting in $d = 0.415$, $g = 0.315$, $T_L = 1.833$ °C, and $T_U = 24.918$ °C. These growth parameters were estimated from laboratory studies with salmon reared in conditions that are likely unrepresentative of conditions in the field (e.g. *ad libitum* rations), and thus may underestimate thermal impacts. For example Childress and Letcher (2017) found that thermal performance curves for brook and brown trout in the field were reduced by ~2-3°C in the field compared to laboratory studies. Martin et al. (2017) found a similar shift in thermal tolerance for Chinook winter-run embryos from lab to field. Following Childress and Letcher (2017) and Martin et al. (2017), we applied a temperature correction factor, $T_{corr} = 3.0$ °C. To account for differences in laboratory vs. field ration levels, we also included the feeding level *Food*, the

fraction of the maximum growth rate due to food limitation (*ad libitum* = 1), The relative growth rate (100 * Ω/ Ω_{max}) was calculated at spatial and temporal locations.

A smolting threshold appears to exist, whereby resident juveniles need to reach a size of approximately 6g in order to successfully smolt and outmigrate (Ewing et al. 1979, Larsen and Beckman 2010, Sharron 2015), meaning that resident juveniles need to remain in-stream until they reach this size. We assumed that chinook fry emerged with mass 0.46 g, based on the relationship between the mass of eggs and emergent fry and an average chinook egg weight of 300 g (Beacham and Murray 1990, Quinn 2018), and calculated daily mass based on the temperature-dependent growth rate until the smolt size threshold was reached:

$$M_{t+1} = M_t + \frac{\Omega}{100} * M_t^{1-\alpha}$$

where M_t is the previous mass, M_{t+1} is the new calculated mass, Ω is the mass-standardized growth rate from above, and α is the allometric growth constant, calculated as 0.338 for juvenile chinook (Perry et al. 2015).

Juvenile mortality is high in-stream primarily due to predation, and mortality rates are strongly size-dependent, putting immense pressure on small fish to grow quickly and outmigrate (Lorenzen 1996). To calculate a daily survival probability (S_{t+1}), we assumed a daily background mortality rate (X_u) at the current calculated mass of the fish (M_t) (Peterson and Wroblewski 1984, Lorenzen 1996):

$$S_{t+1} = S_t * \exp(X_u * M_t^f)$$

where S_t is the previous survival probability, X_u is the background mortality rate per 1 g of fish, and f is the allometric scaling factor. For salmonids in natural systems, Lorenzen (1996) calculated X_u = 2.75 y^{-1} (or 2.75/365.25 d^{-1}) and f = -0.27.

The daily mass and survival probability until smolt size was reached was calculated based on daily temperature within the river. In optimum field conditions where juveniles always experienced the maximum growth rate (i.e. $T \sim 16$ C), juveniles reach smolt size in 83 days and have a maximum survival of 62%. We present our results as survival at a given thermal exposure as a percent of the maximum survival to smolt size that would occur at optimum temperatures.

Comparison of thermal effects across life stages and scenarios

We applied each model to the spatial-temporal temperature matrix for each river in R. To assess thermal effects across life stages, we compared 1) likelihood of successful spawning, 2) egg-to-fry survival, and 3) relative smolting success. To help elucidate if a life stage's actual phenology and/or spatial locations mitigate negative thermal effects, we compared nonweighted and weighted results. Nonweighted results treated each spatial-temporal location as equally likely, assuming that a life stage could occur everywhere in equal relative abundance throughout the year. For weighted results for each life stage, a random spatial-temporal location was pulled from the spatial and phenological distributions (i.e. arrival, spawn, or emergence timing and spawning locations) for 1000 replicates. Density plots were then created, where each result in space and time represents one observation.

RESULTS

Clear Creek

Spring-run chinook in Clear Creek hold for an average of 112 days prior to spawning (Table 2, Supp. Fig. S2.1A). Peak arrival occurs in June, but salmon have been seen entering Clear Creek in March (CCTT 2017). Spawning is constrained to a few short weeks, with the majority of spawning occurring in the latter half of September and the first week of October. In comparison, fall-run hold for an average of 18 days in-river and peak spawning occurs in early November (Table 2, Supp. Fig. S2.1B). Spring-run spawn uniformly from the weir upstream of river km 12 to the Whiskeytown Dam at river km 29, whereas fall-run spawning habitat follows a normal distribution, peaking around river km 8 (Table 3, Supp. Fig. S3.1).

Metabolic expenditure of holding adults was influenced both by duration of holding time and spatial location (Fig. 3A). Spring-run salmon holding downstream in warmer temperatures expended more energy than those holding upstream, whereas fall-run holding costs were predicted to be similar upstream and downstream. There were significant costs associated with spring-run arriving prior to ~mid-May, such that our model calculated that most fish arriving before then would have no energy to allocate to spawning. Peak arrival, however, occurs in early June (Table 2, Fig. S2.1A). Similarly, fall-run arriving before ~mid-September would likely expend to much energy during holding to spawn, but peak arrival occurs mid-October (Table 2, Fig. S2.1B). By randomly sampling spawning date (1000 replicates), we calculated likely holding times based on arrival date, and ran our energy expenditure model for each replicate; the standard deviation was low for all locations in space and time (max: 0.419; Fig. S4.1).

High egg-to-fry mortality was predicted for eggs spawned from ~mid-February through September downstream or mid-April through August upstream (Fig. 3B). There was a steep gradient of high-to-low mortality upstream in late-August to early September, coinciding with the temperature dropping to below 15°C. A shallower gradient of low-to-high mortality, beginning in March downstream and May upstream, coincided with temperatures consistently rising above 11°C.

Juveniles grew at high temperature-dependent rates throughout most of the year along the entirety of Clear Creek (Fig. 3C). Spring-run fry rear throughout the entire creek from November-March, whereas fall-run fry rear in the downstream 13.5 km from January-April. Larger juveniles (> 60 mm) rear from April-August for spring-run and May-September for fall-run (AFRP 2015).

A comparison of thermal effects across life stages revealed that holding spring-run adults experienced high holding costs that may have reduced their ability to spawn successfully or lowered egg condition in 2013 (Fig. 4A). In contrast, most fall-run did not have high costs from holding (Fig. 4B). Overall, fall-run showed higher success for each life stage when compared to spring-run. Juveniles experienced relatively high likelihood to reach smolt size, and egg-to-fry survival was usually > 50%. For Chinook in Clear Creek in 2013, temperature most negatively affected spring-run holding adults, with all other life stages for both spring- and fall-run experiencing relatively high success.

Stanislaus River

Fall-run spawned an average of 23 days after arriving to the Stanislaus River (Table 2, Supp. Fig. S2.2). Spawning peaked in late-November, but new redds were observed until mid-December (Table 2). Note that this distribution is based on a single year of redd surveys and may shift with additional years.

Based on the phenological and spatial distributions for each life stage, smolt success is high, spawning success is fairly high, and egg-to-fry survival is low (Fig. 4C). Our model predicts that most spawners arriving prior to ~mid-October will expend too much energy during holding to spawn, although fall-run begin arriving in low numbers as early as mid-September (Fig. 5A, Table 2). Although spawning only occurs in the upper half of the Stanislaus River, our model reveals low holding costs downstream of spawning grounds. Similarly, there is a narrow spatial-temporal window of low egg-to-fry mortality, from late-October to mid-December in the downstream reaches of the Stanislaus River where spawning does not occur (Fig. 5B). The ~15 km below the Goodwin Dam, where spawning does occur, have suitable thermal habitat for a much longer period of time, from late-October to ~early April. Juveniles are likely to smolt throughout most of the river for most of the year. However, a lower likelihood (<70%) occurs from ~March-September in the downstream reaches (Fig. 5C).

Tuolumne River

Because of the similarity in thermal profiles for the Tuolumne and Stanislaus Rivers (Fig. 2) and because we used Stanislaus River phenology in modeling for the Tuolumne River for this Draft, results for the Tuolumne River are similar to that of the Stanislaus River (Fig. 4, Fig. 6). The primary difference is that egg-to-fry survival shows two distinct regions, one with very high survival and one with ~50% predicted survival. However, results may change with the application of Tuolumne-specific phenology and spatial data.

DISCUSSION
Thermal effects within and between Central Valley rivers

Here we illustrate a framework to compare temperature-dependent thermal effects on different salmonid life stages and runs in three Central Valley rivers. Our results from Clear Creek reveal that spring-run are more thermally stressed than fall-run overall, especially during the long holding period before spawning. Spring-run peak arrival occurs in June, but they can arrive as early as March. Our model showed that these early arrivals experienced high temperatures and expended a lot of energy to sustain their maintenance metabolism, such that they would not have enough energy to spawn. Our framework predicted the most negative thermal effects during holding for all rivers examined (Fig. 4). The metabolic expenditure model shows that fish arriving later have more energy to allocate to spawning, increasing the likelihood of successful spawning. However, our model does not include costs associated with migration. High water temperatures during the summer likely prevent migration, meaning salmon must migrate in the spring before temperatures warm or in the fall after temperatures cool. Future applications of our framework could include a temperature- or flow-dependent energy costs during migration.

Spring-run in Clear Creek are more thermally stressed than fall-run. Dams cut off most of the spring-run spawning habitat, so they are currently spawning in regions that are probably not ideal. The sub-optimal thermal habitat of spring-run may explain their decline and threatened status, and the extirpation of many Central Valley spring-run populations. Although we did not directly test for the spring-run potential along the Stanislaus and Tuolumne Rivers, these rivers

experience warmer temperatures than Clear Creek. If spring-run Chinook were reintroduced, they would likely be more thermally stressed than fall-run in the same rivers.

Due to similar thermal profiles, the Stanislaus and Tuolumne Rivers had similar predicted results (Fig. 5, Fig. 6). The Tuolumne River had the least amount of thermally suitable habitat followed closely by the Stanislaus River. Clear Creek had the most thermally suitable habitat, perhaps explaining why spring-run are viable there. Unlike Clear Creek, the metabolic expenditure during holding was similar upstream and downstream.

Limitations of our approach

The relationship between energy spent during migration, speed of migration, and distance is complex and not well-studied, especially regarding differences between populations and runs. For our model, we assume that spring-run use the same amount of energy as fall-run migrating similar distances (e.g. Martin et al. 2015), but this has not been studied. Our model also does not include a temporal-based account of energy expenditure. Fish migrating closer to spawning time must migrate more quickly, expending larger amounts of energy. Bowerman et al. (2017) calculated that South Fork Salmon River spring-run expend ~4.6 MJ kg^{-1} during migration, but this population travels further and, their calculated costs included some holding time. The value for E_M (energy spent during migration, not including holding or gonad allocation), as with the other parameters, can be altered with additional information or tailored to a specific population.

It's difficult to calculate spawning costs, i.e. how much energy an adult expends digging redds and defending territories. Bowerman et al. (2017) calculated that 8.5% of initial muscle energy stores are used for spawning costs, but this value probably includes gonad allocation costs as well. To directly calculate spawning costs, the difference between the energy density of gonads and muscle needs to be examined for spawn-ready and postspawned individuals.

The calculation of spawning success assumes that several of the parameters are inflexible, such as the amount of energy allocated to gonad development. However, it is unclear if this is actually the case. For example, in sockeye salmon, fecundity, i.e. the number of eggs spawned, seems to be set prior to migration onset, such that any increase in energy expenditure during migration or holding would result in lower egg quality rather than a decreased quantity (Patterson et al. 2004). This may imply that salmon might be able to decrease the amount of energy allocated to gonads when stressed. Smaller salmonid eggs are correlated with smaller fry, increased predation rates, decreased survival, and overall lower fecundity (Bouck et al. 1975, Holtby et al. 1989, Berman 1990, Kinnison et al. 2001).

We assumed that adults held in the same place that they spawned, based on spawning spatial locations. However, Chinook salmon have been shown to hold in cooler refuges, migrating to spawning grounds only when spawning was imminent (Berman and Quinn 1990, Fullerton et al. 2017). The inclusion of spatial locations of cold-water pools for a river may increase the accuracy of thermal effects on holding adults. For Clear Creek, spring-run adults holding in cool pools would mitigate the negative thermal effects implicated by our results.

The incorporation of phenological and spatial distributions revealed that spawn timing and locations help to mitigate embryo mortality. Spawning and incubation do not occur during times of high mortality; for example, embryonic mortality is predicted to be highest during the summer, but spawning does not begin until the temperatures begin to cool in the late-summer, and emergence concludes before temperatures warm again in the late-spring (Fig. 3). A long-

term study may be able to elucidate if phenology and/or spatial distribution are rigid, or temperature-dependent. These results have important implications for determining when and where cold-water resources should be allocated.

Our models are all temperature-dependent because temperature is the major influence on a fish's health and fecundity, but other factors have also been shown to be important. For salmon during their freshwater lifestages, flow can influence metabolic expenditure of adults migrating and holding. A moderate amount of discharge is critical during incubation to deliver oxygen to developing embryos; too little flow and not enough oxygen circulates through redds. Additionally, low flows are associated with dewatered redds, which have little chance of survival if conditions are too dry (Healey 1991, Bjornn and Reiser 1991). For juveniles rearing in the wild, growth rate is dependent on the amount of food available, but this factor is often not known. Future studies on juvenile growth rate should assess field food availability. Similarly, mortality due to predation or other factors should be included whenever known. Finally, there is a large gap in knowledge of diseases. Although certain infections are known to be temperature-dependent, data is primarily from hatcheries and little field information exists. The key to our framework is the conversion of life stage-specific performance into a common currency that measures survival, so any of the above mentioned factors that affects salmonid performance could be incorporated into our framework if the relationship between the factor and life stage-specific survival is understood.

Conclusion

Our framework is an effective way to calculate thermal impacts on multiple salmonid runs and life stages within a river over time. Managers can use this method to calculate how incremental changes in temperature will affect different life stages, particularly important in areas where cold-water resources are scarce. This approach could also be implemented to assess population viability in currently uninhabited streams, perhaps above dams or at possible sites for reintroductions. Calculating effects on different life stages for specific rivers in the Central Valley is particularly timely as it becomes clearer that populations exhibit temperature-dependent differences and that California populations experience higher temperatures than Pacific Northwest populations. Finally, our framework is relatively simple to implement, can be applied to empirical or theoretical data, and can be changed, altered, or added to as more data or better models become available.

PART 2: TABLES AND FIGURES

Table 1. Description of streams in the Central Valley selected to illustrate our framework and spatial/phenological sources. Temperature monitors are from NorWest. Years are the years we chose to analyze based on the availability of temperature and spatial/phenological data. Length indicates the number of km examined, usually to an impassible fish barrier.

	Clear Creek	Stanislaus River	Tuolumne River
Spring-run	Yes	Extirpated	Extirpated
Fall-run	Yes	Yes	Yes
Late-fall-run	Yes*		
Winter-run	Extirpated	No	No
Temp monitors (n)	14	7	28
Years	2002-2015	1993-2014	1993-2014
Length (km)	29	93	86
Mean annual flow	Low	Moderate	High
Spring-run arrivals	Video monitor[9]	NA	NA
Fall-run arrivals	Video monitor[3,4,5,6,7]	Video monitor[11]	Video monitor[11]
Spring-run spawning	Redd counts[8]	NA	NA
Fall-run spawning	Redd counts[10]	Redd counts[11]	
Juvenile rearing	Verbal[1], Rotary screw trap[2]		

*low numbers and not well-documented
[1]CCTT 2016, [2]Earley et al. 2013, [3]Killam and Johnson 2013, [4]Killam et al. 2014, [5]Killam et al. 2015, [6]Killam et al. 2016, [7]Killam et al. 2017, [8]RBFWO, Provins pers.comm., [9]CCTT 2017, [10]Meneks 2017, [11]Tsao and Murphey, pers. comm., 2018

Table 2. Summary statistics of the empirical phenological datasets. Values are in Julian day.

Population	Mean	SD	Median	Min	Max	Skewness	Kurtosis
Clear Creek spring-run arrival	164	26.5	152	91	243	0.25	3.83
Clear Creek spring-run redd	276	10.9	280	238	322	0.73	4.5
Clear Creek fall-run arrival	289	15	288	245^	349*	0.23	3.10
Clear Creek fall-run redd`	307	7.9	308	287	329	-0.10	3.08
Stanislaus River fall-run arrival	308	18.1	308	259^	350*	0.08	2.76
Stanislaus River fall-run redd	331	11	329	287	350	-0.06	2.28
Tuolumne River fall-run arrival^^							
Tuolumne River fall-run redd^^							

`note that spawning phenology based on nearby Scott River
^earlier observations removed due to potential misidentification
*later observations removed because no new redds observed
^^for this Draft, we applied Stanislaus River phenology to the Tuolumne River

Table 3. Summary statistics of the empirical spatial datasets. Values are in river kilometer, where '0' is the river mouth.

Population	Mean	SD	Median	Min	Max	Skewness	Kurtosis

Clear Creek spring-run redd	20.83	5.12	20.5	12.5	29.5	0.057	1.59
Clear Creek fall-run redd	7.98	1.63	8.5	3.5	10.5	-0.635	2.89
Clear Creek spring-run rearing^	NA	NA	NA	0	29.5	NA	NA
Clear Creek fall-run rearing^	NA	NA	NA	0	13.5	NA	NA
Stanislaus River fall-run redd[3]	NA	NA	NA	52.6	92	NA	NA
Stanislaus River fall-run rearing	NA	NA	NA	0	92	NA	NA
Tuolumne River fall-run redd`							
Tuolumne River fall-run rearing`							

^based on description only, not quantified data
`for this draft, based on description only, not quantified data

---

[3] Note that Stanislaus River redd surveys are based on verbal descriptions and are thus sampled from a uniform distribution for this Draft. We expect to have redd survey location data for the Final report.
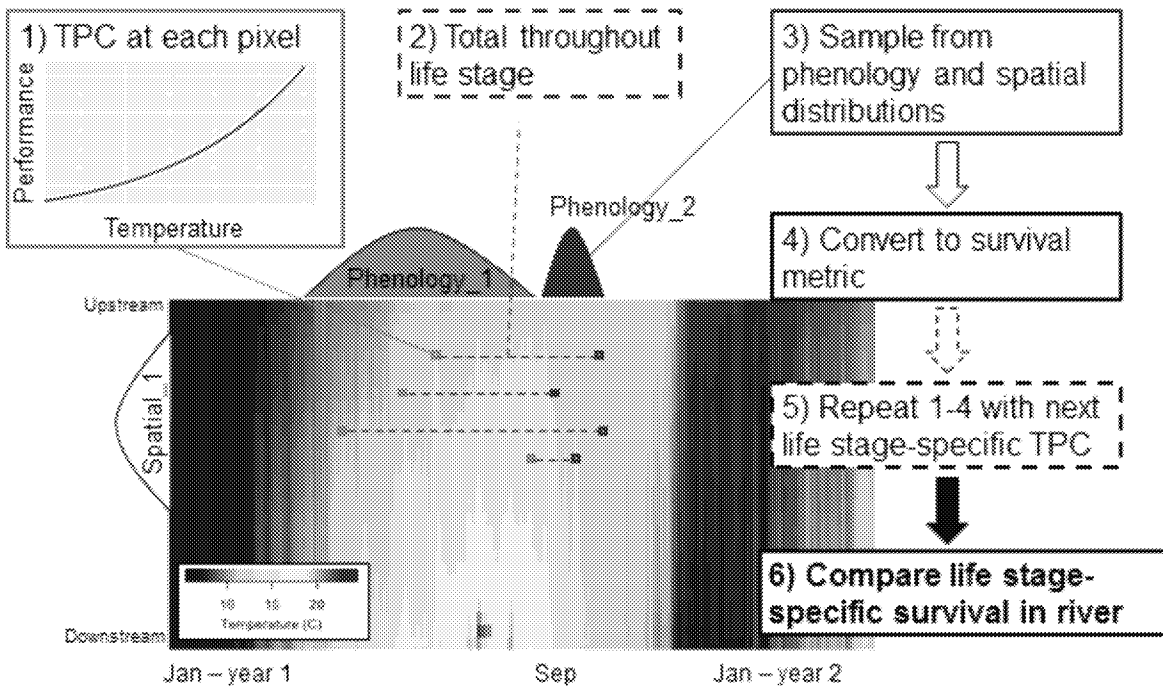
Figure 1. Illustrated framework for assessing thermal impacts of life stages along a river. 1) First, the life stage-specific thermal performance curve model (TPC) is run at each spatial/temporal location, with temperature as the input. The example TPC shown is based on energy expenditure of adults during holding. 2) Based on known phenology, the total performance throughout the duration of the life stage is calculated. In the example shown, Phenology_1 is arrival timing and Phenology_2 is spawn timing, and duration of holding is calculated based on these distributions. 3) Results are sampled from the phenology and spatial distributions to estimate performance at spatial/temporal locations where salmon are found, as opposed to the whole river throughout the year. 4) To compare life stages, performance is converted into a metric of survival. For example, energy expenditure during holding is converted into ability to successfully spawn based on energy use. 5) The next life stage-specific TPC is applied. 6) Finally, thermal impacts of different life stages are compared.